Molecular Microbiology

WILEY

RESEARCH ARTICLE OPEN ACCESS

The Impact of YabG Mutations on *Clostridioides difficile* Spore Germination and Processing of Spore Substrates

Morgan S. Osborne[1] | Joshua N. Brehm[1] | Carmen Olivença[2] | Alicia M. Cochran[1] | Mónica Serrano[2] | Adriano O. Henriques[2] | Joseph A. Sorg[1]

[1]Department of Biology, Texas A&M University, College Station, Texas, USA | [2]Instituto de Tecnologia Química e Biológica, Universidade Nova de Lisboa, Oeiras, Portugal

Correspondence: Joseph A. Sorg (jsorg@bio.tamu.edu)

Received: 24 May 2024 | **Revised:** 27 August 2024 | **Accepted:** 30 August 2024

Funding: This project was supported by awards 5R01AI116895 and 5R01AI172043 to J.A.S. from the National Institute of Allergy and Infectious Diseases.

Keywords: *Clostridioides difficile* | germination | protease | spore | YabG

ABSTRACT

YabG is a sporulation-specific protease that is conserved among sporulating bacteria. *Clostridioides difficile* YabG processes the cortex destined proteins preproSleC into proSleC and CspBA to CspB and CspA. YabG also affects synthesis of spore coat/exosporium proteins CotA and CdeM. In prior work that identified CspA as the co-germinant receptor, mutations in *yabG* were found which altered the co-germinants required to initiate spore germination. To understand how these mutations in the *yabG* locus contribute to *C. difficile* spore germination, we introduced these mutations into an isogenic background. Spores derived from *C. difficile yabG*$_{C207A}$ (a catalytically inactive allele), *C. difficile yabG*$_{A46D}$, *C. difficile yabG*$_{G37E}$, and *C. difficile yabG*$_{P153L}$ strains germinated in response to taurocholic acid alone. Recombinantly expressed and purified preproSleC incubated with *E. coli* lysate expressing wild type YabG resulted in the removal of the presequence from preproSleC. Interestingly, only YabG$_{A46D}$ showed any activity toward purified preproSleC. Mutation of the YabG processing site in preproSleC (R119A) led to YabG shifting its processing to R115 or R112. Finally, changes in *yabG* expression under the mutant promoters were analyzed using a SNAP-tag and revealed expression differences at early and late stages of sporulation. Overall, our results support and expand upon the hypothesis that YabG is important for germination and spore assembly and, upon mutation of the processing site, can shift where it cleaves substrates.

1 | Introduction

Susceptibility to *Clostridioides difficile* infection (CDI) is commonly associated with the use of broad-spectrum antibiotics that disrupt the normally protective colonic microbiota (Theriot et al. 2014; Buffie et al. 2015; Di Bella et al. 2024). Subsequent ingestion of *C. difficile* spores results in the germination of the spore form to the toxin-producing vegetative form (Paredes-Sabja, Shen, and Sorg 2014). *C. difficile* vegetative cells secrete two toxins that damage the colonic epithelium—resulting in the symptoms associated with CDI (e.g., diarrhea or pseudomembranous colitis) (Smits et al. 2016). Because spores are metabolically dormant and resist antibiotic action/harsh environmental conditions, they are the dispersive and transmissive form of the organism (Deakin et al. 2012). Unfortunately, the primary treatment for CDI is additional broad-spectrum antibiotics (e.g., vancomycin or fidaxomicin) (Zar et al. 2007). Though these antibiotics treat the toxin-producing vegetative cells, but not the dormant spores, they continue to disrupt the colonic microbiota and can leave the patient susceptible to reinfections (Smits et al. 2016). Approximately 15–20% of patients experience recurring disease, and the likelihood of subsequent episodes increases with each recurrence (Di Bella et al. 2024).

C. difficile spores germinate in response to certain host-derived bile acids (e.g., taurocholic acid) and amino acids (e.g.,

glycine) (Shrestha and Sorg 2018; Sorg and Sonenshein 2008, 2009; Howerton, Ramirez, and Abel-Santos 2011; Ramirez, Liggins, and Abel-Santos 2010; Bhattacharjee, McAllister, and Sorg 2016; Shrestha, Lockless, and Sorg 2017; Wilson 1983; Wilson, Kennedy, and Fekety 1982). Prior work provided genetic evidence that CspC is the bile acid germinant receptor and CspA is the co-germinant (amino acid) receptor (Francis et al. 2013; Shrestha, Cochran, and Sorg 2019; Kevorkian and Shen 2017; Rohlfing et al. 2019). Despite the absence of a catalytic triad in these subtilisin-like proteases, these two pseudoproteases regulate *C. difficile* spore germination (Kevorkian and Shen 2017; Kevorkian, Shirley, and Shen 2016; Shrestha, Cochran, and Sorg 2019; Francis et al. 2013). Interestingly, CspA is encoded as a translational fusion to CspB (CspBA) and CspC is encoded downstream in the same operon (Paredes-Sabja, Setlow, and Sarker 2011; Bhattacharjee, McAllister, and Sorg 2016; Adams et al. 2013). CspBA is post-translationally processed to CspB and CspA by the sporulation-specific protease, YabG (Shrestha, Cochran, and Sorg 2019; Kevorkian, Shirley, and Shen 2016; Kevorkian and Shen 2017). In addition to processing CspBA, YabG also cleaves the pre-sequence from preproSleC (a cortex degrading enzyme) to generate proSleC, the form present in mature spores (Shrestha, Cochran, and Sorg 2019; Kevorkian, Shirley, and Shen 2016). We hypothesize that CspB is associated with CspC and CspA in dormant spores, with CspC and CspA inhibiting the proteolytic activity of CspB. Upon binding of the bile acid and co-germinant, CspC and CspA dissociate from CspB. CspB then cleaves the inhibitory pro-peptide from proSleC, resulting in activation of SleC, cortex degradation, and the subsequent steps in germination (Shrestha, Cochran, and Sorg 2019; Zhu, Sorg, and Sun 2018; Adams et al. 2013; Francis, Allen, and Sorg 2015). The absence of *yabG* has also been shown to influence the extractability/expression of coat and exosporium proteins, SpoIVA, CotA, CotE, and CdeM in a *C. difficile yabG* mutant, suggesting other targets of YabG (Marini et al. 2023; Zhu, Sorg, and Sun 2018).

YabG is a conserved sporulation-specific protease. In *Bacillus subtilis*, YabG is important for proper assembly of the spore coat and has been shown to process at least six coat proteins (SpoIVA, CotF, CotT, YeeK, YxeA, and SafA) (Takamatsu, Imamura et al. 2000; Takamatsu, Kodama et al. 2000). Of those proteins, only SpoIVA has an orthologue in *C. difficile* and may be a YabG substrate (Kevorkian, Shirley, and Shen 2016). YabG is produced during sporulation in the mother cell, under the alternative RNA polymerase sigma factors σ^E and σ^K (Fimlaid et al. 2013; Pereira et al. 2013; Saujet et al. 2013; Takamatsu, Kodama et al. 2000). *C. difficile* YabG is required for the expression of two σ^K-dependent genes *cotA* and *cdeM*, which encode a coat and an exosporium protein, respectively (Marini et al. 2023).

Using an ethyl methane sulfonate (EMS) screen to identify strains which germinated without a co-germinant, we previously identified mutations in the *yabG* coding and promoter regions (Figure 1 and Table S3) (Shrestha, Cochran, and Sorg 2019). Moreover, these *yabG* mutant strains incorporated preproSleC and CspBA (the unprocessed forms) into spores. One of the *yabG* mutant alleles, $yabG_{A46D}$, (Table S3) appeared to have lower activity than wild-type, but the data were inconclusive (Shrestha, Cochran, and Sorg 2019).

Here, we quantified the processing abilities of recombinantly expressed *yabG* mutant alleles and determined the in vivo effects on *C. difficile* spore germination. We show that of the previously identified *yabG* alleles, only $YabG_{A46D}$ showed any activity in processing preproSleC. Mutations in the *yabG* locus result in misprocessing of germination proteins and spore coat proteins, whereas mutations in the region upstream of the *yabG* start codon (promoter and Shine-Dalgarno) affected the timing of expression.

2 | Results

2.1 | Expression of $YabG_{A46D}$ Leads to Reduced Processing of preproSleC

YabG cleaves the pre-peptide from preproSleC, with proSleC being incorporated into the mature spore (Shrestha, Cochran, and Sorg 2019; Kevorkian, Shirley, and Shen 2016; Marini et al. 2023). To understand the processing capabilities of the *yabG* EMS mutant alleles previously identified, we recombinantly expressed and purified *C. difficile* preproSleC in *E. coli*. preproSleC was incubated with *E. coli* lysate expressing YabG, $YabG_{C207A}$, $YabG_{A46D}$, $YabG_{P153L}$, or $YabG_{G37E}$ from an IPTG-inducible promoter. Due to expression differences of $YabG_{C207A}$, $YabG_{A46D}$, $YabG_{P153L}$, or $YabG_{G37E}$ in *E. coli* compared to wild type YabG, various amounts of the *E. coli* lysate were incubated with the preproSleC to be equal to that of wild type. We then determined the amount of proSleC present in the sample using immunoblotting and quantified by Li-COR imaging. Lysate expressing wild type YabG efficiently processed preproSleC to proSleC to nearly 100% within 1 h of incubation (Figure 2A and Figure S1A). $YabG_{C207A}$, a catalytically inactive mutant, served as a negative control (Figure 2B and Figure S1B) (Marini et al. 2023). Interestingly, of the mutant alleles, only $YabG_{A46D}$ showed any ability to process preproSleC to proSleC. However, only 65% proSleC was present after 3 h of incubation, suggesting that $YabG_{A46D}$ does not process preproSleC as efficiently as the wild type allele (Figure 2C and Figure S1C). $YabG_{G37E}$ (Figure 2D and Figure S1D) and $YabG_{P153L}$ (Figure 2E and Figure S1E) did not process preproSleC. During our analyses, we noticed the presence of a proSleC even in the absence of exposure to *E. coli* lysate (Figures S1, S2A and S2C). To ensure that the presence of proSleC in these assays was a product of preproSleC purification and not due to processing during incubation with *E. coli* lysate, lysate of *E. coli* BL21(DE3) containing an empty pET22b vector (pEV) was incubated with the purified preproSleC. Processing was compared to the wild type *yabG* allele control (Figures S2B and S2D). Because the abundance of the proSleC form does not increase in the *E. coli* BL21(DE3) pEV control, we conclude that *E. coli* is not processing preproSleC and that the observed proSleC is a degradation product generated during our preproSleC purification. The presence of this product does not change the outcome or conclusions of these assays.

2.2 | YabG Can Shift the Processing Site of preproSleC to Nearby Arginine Residues

We previously identified the YabG processing site of preproSleC to be immediately after R119 using Edman degradation (Shrestha, Cochran, and Sorg 2019). Interestingly, the deletion of

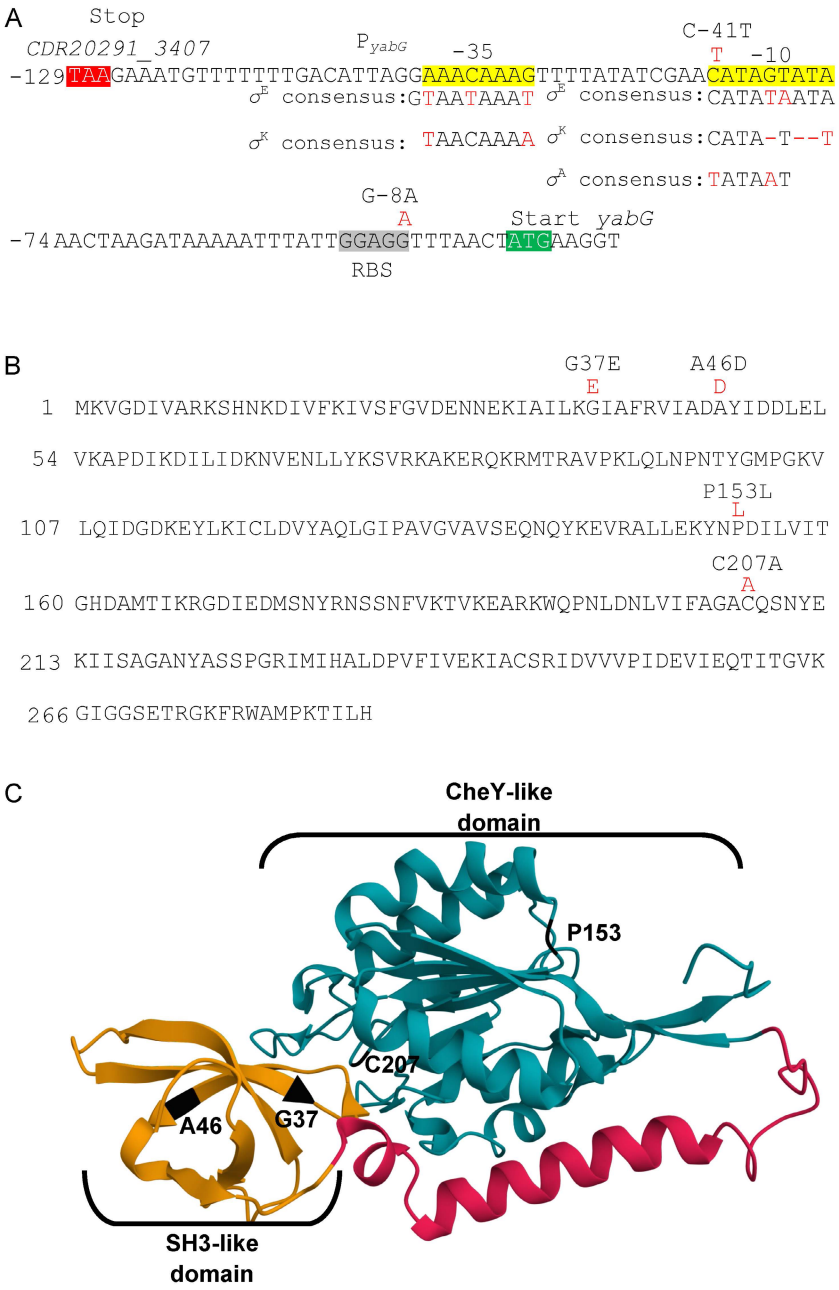

FIGURE 1 | Mutations in the regulatory region of *yabG*. (A) The −10 and −35 regions of the *yabG* promoter, utilized by both σ^E and σ^K in *C. difficile*, are shown in yellow and the consensus for the two σ factors indicated below. The position of the C-41T and G-8A mutations is shown in red; the C-41 T substitution makes the −35 region of the *yabG* promoter closer to the consensus for σ^A recognition (shown below the sequence). The sequence shown corresponds to the fragment fused to the $SNAP^{Cd}$ reporter with numbers indicating the position relative to the *yabG* start codon. (B) The protein coding sequence of *C. difficile* YabG, with mutations, $yabG_{G37E}$, $yabG_{A46D}$, $yabG_{P153L}$, and $yabG_{C207A}$ shown in red. Numbers indicate the position relative to the fMet. (C) Alphafold2 predsdiction of *C. difficile* YabG. G37, A46, P153, and C207 are colored black. The CheY-like domain is colored teal, the linker is pink, and the SH3-like domain is colored yellow.

the identified SRQS sequence resulted in processing of prepro-SleC after R115 and normal incorporation of proSleC into the spores. This suggested that YabG could shift its processing site to a nearby arginine (Shrestha, Cochran, and Sorg 2019). To test the limits of YabG to shift its processing site, we first co-incubated $preproSleC_{R119A}$ with *E. coli* lysate expressing *yabG* (referred to as YabG from hereon), as described above. Because the $prepro-SleC_{\Delta SRQS}$ mutant was processed at R115 instead of R119, we hypothesized that the R119A protein would also be processed at R115 (Shrestha, Cochran, and Sorg 2019). Indeed, the first five amino acids of the resulting proSleC were SFSAQ, suggesting that YabG processed after R115 (Figure 3A). Next, we generated a mutant allele with both arginine amino acids replaced, $preproSleC_{R119A/R115A}$, which YabG processed at R112 (Figure 3A). When a triple substitution was tested, $preproSleC_{R119A/R115A/R112A}$, we observed no processing (Figure 3A). This suggests that YabG processes after arginine residues and that, upon mutation, the processing site shifts within certain limits.

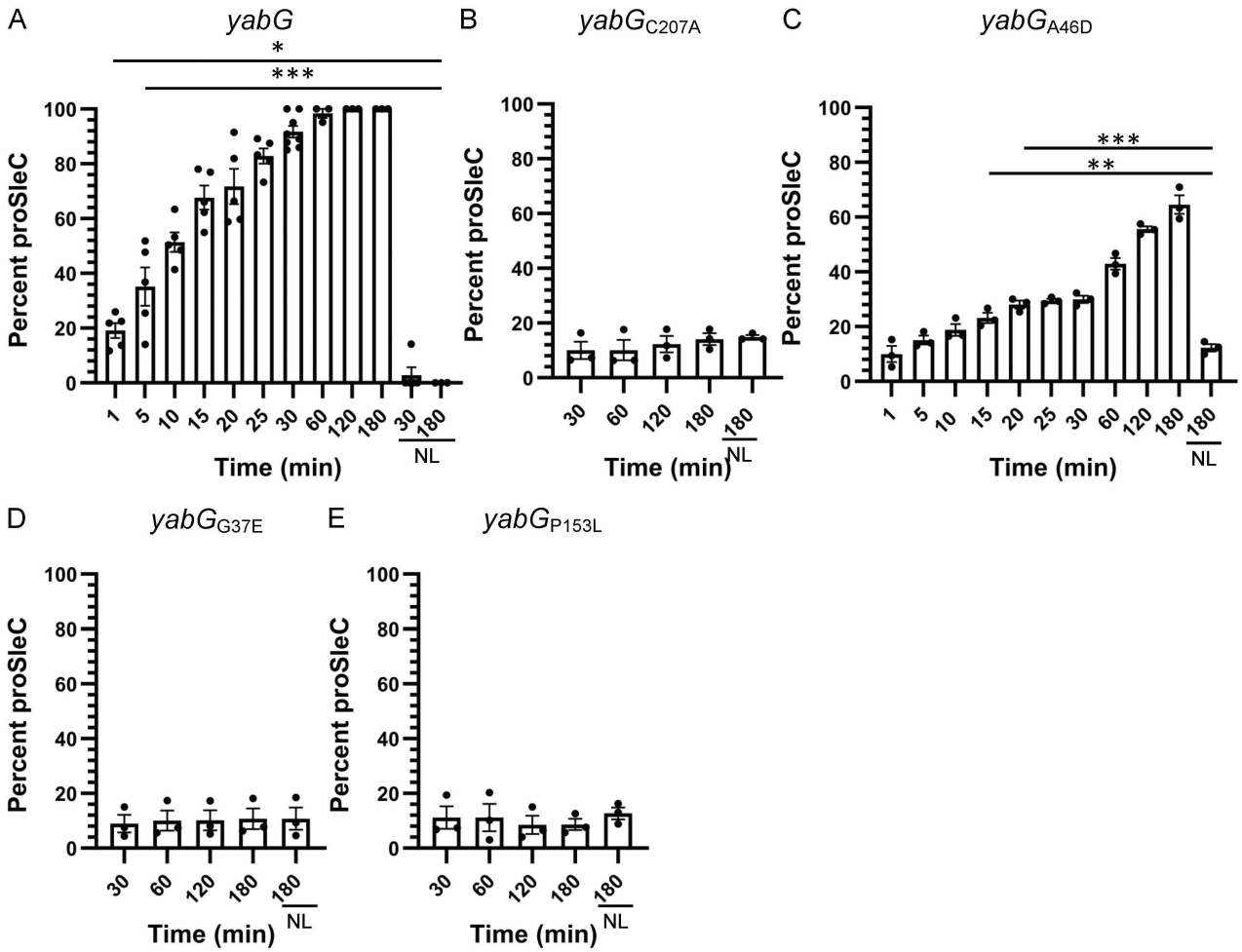

FIGURE 2 | Processing of preproSleC by mutant YabG variants. Percent of proSleC present when incubated with the different *yabG* allele. The percentage of proSleC processed by: (A) Wild type *yabG*, (B) $yabG_{C207A}$, (C) $yabG_{A46D}$, (D) $yabG_{G37E}$, and (E) $yabG_{P153L}$, were quantified on the LI-COR Odyssey-CLx (proSleC signal)/(proSleC signal + preproSleC signal) × 100. (NL) indicates where no *E. coli* lysate was added to purified preproSleC. The data represent the averages from three to eight biological replicates and error bars represent the standard error of the mean. Statistical significance was determined using one-way ANOVA with Šídák's multiple comparisons test (*$p < 0.0332$; **$p < 0.0021$, ***$p < 0.0001$). The purified SleC used in the assays with $yabG_{C207A}$, $yabG_{G37E}$, and $yabG_{P153L}$ had ~15% proSleC present prior to the assay in the sample as seen in the purified preproSleC negative controls (NC).

Because Edman degradation only reveals N-terminal amino acids, it was unknown if YabG was processing at these arginine residues in a sequential manner, that is, at R112, then R115, and lastly R119. To test this hypothesis, $preproSleC_{R112A}$ and $preproSleC_{R112A/R115A}$ were recombinantly expressed, purified, and incubated with YabG. Edman degradation revealed that YabG processed both R115A and R115A/R112A alleles at R119 (Figure 3A). There were also no changes in processing efficiency of YabG on the various preproSleC mutants with the exception of $preproSleC_{R112A/R115A/R119A}$, which was not processed. Using an AlphaFold2 prediction of the preproSleC protein structure, we noticed that the three arginine residues at which YabG processes are in a disordered region (Figure 3B) (Varadi et al. 2024; Jumper et al. 2021). Surprisingly, there is another arginine, R110, within this region that was not cleaved by the YabG in any of our assays. Some AlphaFold2 models predict that the R110 is located within a beta sheet, suggesting that YabG only processes after arginine residues found in the disordered loops (Figure 3B). Alternatively, the presence of a proline at position 109 could be excluding YabG from processing at R110.

2.3 | Mutations in yabG Result in a TA Only Germination Phenotype

YabG processes two proteins involved in *C. difficile* spore germination: preproSleC and CspBA (Shrestha, Cochran, and Sorg 2019; Kevorkian, Shirley, and Shen 2016). In prior work, we found that a *C. difficile yabG::ermB* mutant germinated in the presence of taurocholic acid (TA) alone and did not respond to the addition of a co-germinant (Shrestha, Cochran, and Sorg 2019). To determine if the mutations in *yabG* affected the ability to respond to co-germinants, isogenic mutants were made of $yabG_{A46D}$, $yabG_{G37E}$, $yabG_{P153L}$, $yabG_{C207A}$, $yabG_{C\text{-}41T}$, and $yabG_{G\text{-}8A}$ in a *C. difficile* R20291 Δ*pyrE* strain. Spores derived from the indicated strains in buffer alone did not germinate (Figure 4A,D). Wild type *C. difficile* Δ*pyrE* does not germinate with the addition of TA alone (Figure 4B,E) and requires a co-germinant (glycine) to germinate (Figure 4C,F). However, spores derived from the *C. difficile* Δ*pyrE* $yabG_{C207A}$, *C. difficile* Δ*pyrE* $yabG_{A46D}$, *C. difficile* Δ*pyrE* $yabG_{P153L}$, and *C. difficile* Δ*pyrE* $yabG_{G37E}$ strains germinated with the addition

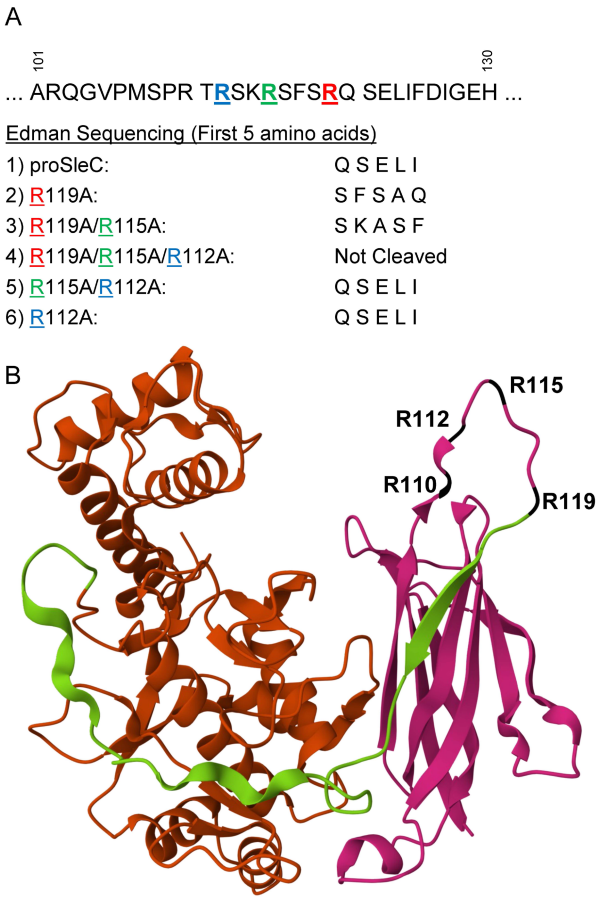

FIGURE 3 | Processing site of recombinant preproSleC by *yabG* alleles. (A) Recombinantly expressed and purified preproSleC, preproSleC$_{\Delta SRQS}$, preproSleC$_{R119A}$, preproSleC$_{R119A/R115A}$, preproSleC$_{R119A/R115A/R112A}$, preproSleC$_{R115A/R112A}$, and preproSleC$_{R112A}$ were incubated with *E. coli* lysate expressing YabG. The N-terminus of the YabG-cleaved preproSleC (proSleC) was determined by Edman sequencing. Arginine after which YabG processes preproSleC are colored at position 119 (red), 115 (green), and 112 (blue). (B) *C. difficile* 630Δ*erm* SleC AlphaFold2 protein structure prediction. Highlighted are R110, R112, R115, and R119 in black. The pre-peptide is colored pink, the pro-domain is colored green, and active SleC is colored orange.

of TA but no co-germinant (Figure 4B). Spores derived from the *C. difficile* Δ*pyrE yabG*$_{G\text{-}8A}$ and *C. difficile* Δ*pyrE yabG*$_{C\text{-}41T}$ mutant strains also germinated in the presence of TA alone (Figure 4E). Germination of all the *C. difficile yabG* mutant spores was not enhanced by the addition of glycine (Figure 4C,F). Together these results support the previous findings that these mutations in *yabG* result in spores that no longer respond to co-germinants for germination.

2.4 | Mutations in yabG Affect the Abundance of YabG Processed Proteins

YabG is required for the expression of CotA and CdeM, a coat and an exosporium protein, respectively (Marini et al. 2023). In a *C. difficile yabG* mutant, these proteins have reduced abundance, and the spore has morphological changes (Marini et al. 2023). To investigate if our *C. difficile yabG* mutant alleles also exhibit changes to cortex/coat/exosporium protein abundance, we performed western blots on spore extracts. YabG was detected in the spore extracts of *C. difficile* Δ*pyrE yabG*$_{G37E}$, *C. difficile* Δ*pyrE yabG*$_{A46D}$, *C. difficile* Δ*pyrE yabG*$_{P153L}$, and *C. difficile* Δ*pyrE yabG*$_{C207A}$. *C. difficile* Δ*pyrE yabG*$_{C207A}$ spores exhibited the highest amount of YabG, consistent with previous findings that it does not autoprocess (Figure 5A) (Marini et al. 2023). Of the three single amino acid substitution mutants, *C. difficile* Δ*pyrE yabG*$_{P153L}$ showed the highest abundance of YabG, followed by *C. difficile* Δ*pyrE yabG*$_{G37E}$, and *C. difficile* Δ*pyrE yabG*$_{A46D}$ (Figure 5A). *C. difficile* Δ*pyrE yabG*$_{P153L}$ and *C. difficile* Δ*pyrE yabG*$_{G37E}$ had an abundant processed proSleC, differing from in vitro assays. YabG was not detected in spore extracts derived from the wildtype, *C. difficile* Δ*pyrE yabG*$_{G\text{-}8A}$, and *C. difficile* Δ*pyrE yabG*$_{C\text{-}41T}$ mutant strains. This likely results from YabG auto-proteolytic activity combined with reduced expression in the *yabG*$_{G\text{-}8A}$ and *yabG*$_{C\text{-}41T}$. Compared to wildtype, we also detected a greater abundance of the preproSleC form in all mutants tested (Figure 5A).

CdeM and CotA were absent from spores derived from the *yabG*$_{C207A}$ strain (Figure 5A,B). We also observed less CdeM in spores of *C. difficile* Δ*pyrE yabG*$_{C\text{-}41T}$, *C. difficile* Δ*pyrE yabG*$_{G\text{-}8A}$, and *C. difficile* Δ*pyrE yabG*$_{G37E}$ (Figure 5A). There was no effect on the observed CdeC (Figure 5B). The abundance of cleaved CotE was also reduced in all mutant strains. The *C. difficile* Δ*pyrE yabG*$_{A46D}$ strain had increased processing compared to the other mutant strains. This is consistent with this allele retaining some activity against preproSleC (Figure 2C) (Shrestha, Cochran, and Sorg 2019). Finally, the autoprocessed form of CspB was also detected in all of the mutant spore extracts, consistent with previous findings in spores derived from a *C. difficile* Δ*yabG* mutant strain (Figure 5B) (Kevorkian, Shirley, and Shen 2016).

2.5 | Mutations in yabG Affect the Spore Morphology

To understand if spore assembly was affected in the mutant strains, we imaged the spores by transmission electron microscopy (TEM). In spores derived from the *C. difficile yabG*$_{C207A}$ mutant, a loose connection between the cortex and coat layers is occasionally seen (Figure 6) (Marini et al. 2023). Also, the spore surface lacks electron density or has a very thin electron dense exosporium which lacks bumps; the appendage, when present, is not electron dense but rather shows a lamellar structure (Figure 6). In *C. difficile* Δ*pyrE yabG*$_{P153L}$, *C. difficile* Δ*pyrE yabG*$_{A46D}$ and *C. difficile* Δ*pyrE yabG*$_{G37E}$ spores, the exosporium was thin, and, when present, the bumps were much smaller than in the wild type; the appendage region was less electron dense than in the wild type and showed a lamellar pattern (Figure 6). Spores of the *C. difficile* Δ*pyrE yabG*$_{G\text{-}8A}$ and *C. difficile* Δ*pyrE yabG*$_{C\text{-}41T}$ strains appeared similar. These observations are consistent with the idea that construction of the electron dense outer layer of the spore body and appendage is dependent on CdeM (Marini et al. 2023). In the strains which we observed a reduction in the electron density of the exosporium, we also observed a lower abundance of CdeM in the spore (Figure 5A), consistent with this hypothesis. In all the spores, filamentous projections

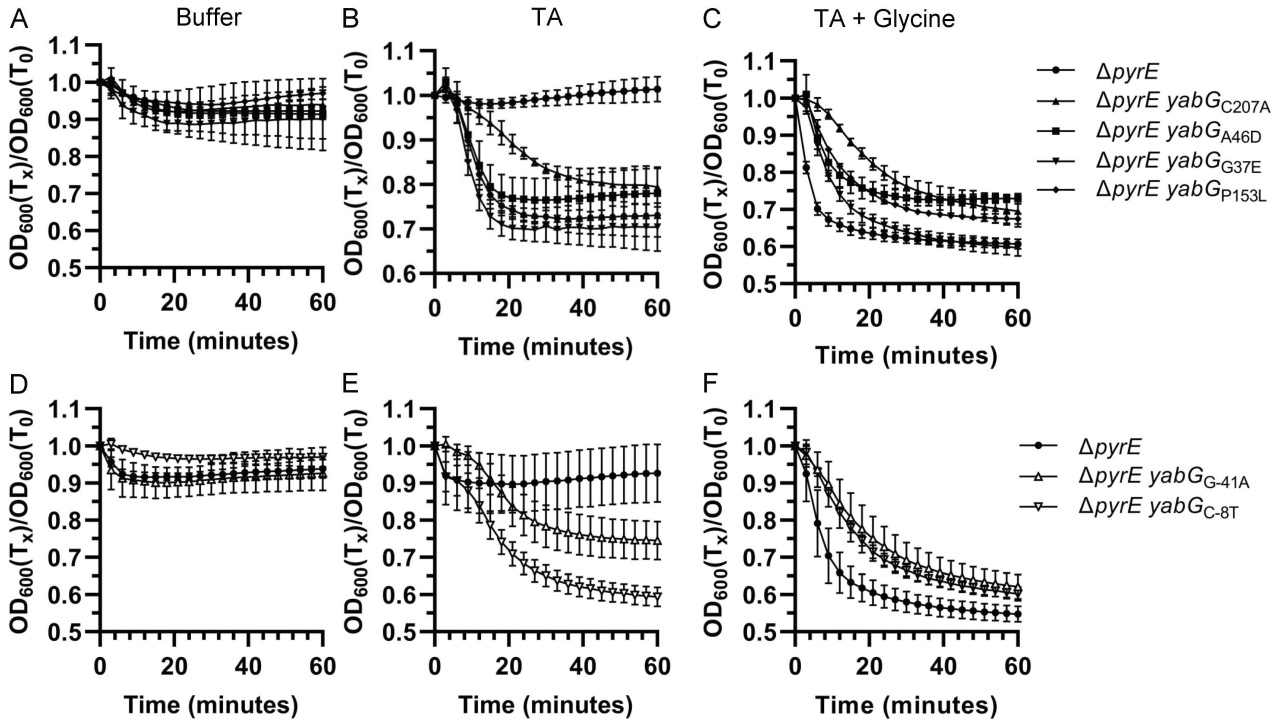

FIGURE 4 | Mutations in YabG allow for germination in the presence of taurocholic acid only. Spores derived from *C. difficile* Δ*pyrE*, *C. difficile* Δ*pyrE*; $yabG_{C207A}$, *C. difficile* Δ*pyrE*; $yabG_{A46D}$, *C. difficile* Δ*pyrE*; $yabG_{P153L}$, *C. difficile* Δ*pyrE*; $yabG_{G37E}$, *C. difficile* Δ*pyrE*; $yabG_{C-8T}$, and *C. difficile* Δ*pyrE*; $yabG_{G-41A}$ germinate in the presence of taurocholic acid alone and do not require a co-germinant. Five microliter of $OD_{600} = 100$ spores derived from *C. difficile* Δ*pyrE* (circles), *C. difficile* Δ*pyrE* $yabG_{C207A}$ (triangle), *C. difficile* Δ*pyrE* $yabG_{A46D}$ (square), *C. difficile* Δ*pyrE* $yabG_{P153L}$ (diamond), *C. difficile* Δ*pyrE* $yabG_{G37E}$ (inverted triangle), *C. difficile* Δ*pyrE*; $yabG_{C-8T}$ (inverted open triangle), and *C. difficile* Δ*pyrE*; $yabG_{G-41A}$ (open triangle) were added to 95 μL germination buffer. (A and D) Strains were suspended in buffer alone, (B and E) in buffer supplemented with 10 mM TA, or (C and F) in buffer supplemented with 10 mM TA and 30 mM glycine. Germination was monitored at OD_{600}. Data points represent the averages from biological triplicate experiments and error bars represent the standard error of the mean.

are seen emanating from the spore surface, which may correspond to the structures formed by the Bcl proteins (Pizarro-Guajardo et al. 2014, 2020; Paredes-Sabja, Shen, and Sorg 2014).

2.6 | Characterizing the Effects of yabG Promoter Mutations on *yabG* Expression

To study the timing of *yabG* expression during sporulation, the fragment derived from the *C. difficile yabG* regulatory region (Figure 1A) was fused to the $SNAP^{Cd}$ reporter. In the $SNAP^{Cd}$ constructs, the *C. difficile yabG* RBS was fused to the start codon of the reporter so that mutations presumably affecting transcription (*C. difficile* Δ*pyrE* $yabG_{C-41T}$) or translation (*C. difficile* Δ*pyrE* $yabG_{G-8A}$) could be assessed (Figure 7A). These experiments were conducted in *C. difficile* 630Δ*erm* due to better data on the timing of *C. difficile* sporulation in this strain (Marini et al. 2023). As observed previously, the wild type promoter is active during late stages of sporulation, mainly in sporangia of phase gray/phase bright spores (Figure 7A, white arrows) (Marini et al. 2023). The *C. difficile* Δ*pyrE* $yabG_{C-41T}$ mutation increases expression of the reporter earlier than the wild type (when the forespore is not yet discernible by phase contrast microscopy) (Figure 7A, black/gray arrows) and expression is reduced in sporangia at late stages in sporulation (Figure 7A, white arrows). In contrast, in the *C. difficile* Δ*pyrE* $yabG_{G-8A}$ mutant, production of the reporter had undetectable levels of expression at all stages of sporulation (Figure 7A).

We next quantified the level of expression in sporangia of phase gray/phase bright spores of wild type *C. difficile* Δ*pyrE*, *C. difficile* Δ*pyrE* $yabG_{G-8A}$, and *C. difficile* Δ*pyrE* $yabG_{C-41T}$ strains at various stages (early, phase dark, and phase bright) of sporulation (Figure 7B). Consistent with observations in Figure 7A, we observed $yabG_{C-41T}$ expression earlier than other strains. $yabG_{C-41T}$ expression was lower in abundance at later stages of sporulation (Figure 7B) compared to wild type, with the $yabG_{G-8A}$ allele showing the lowest expression in all stages of sporulation (Figure 7B). These results are consistent with the germination data shown in Figure 4E, in which germination occurs in the presence of TA alone as well as the immunoblot in Figure 5A, where yabG is not observed in either of these mutant strains.

3 | Discussion

Previous work on YabG has focused mostly on *Bacillus subtilis* (Takamatsu, Imamura et al. 2000; Takamatsu, Kodama et al. 2000; Kuwana et al. 2006; Yamazawa et al. 2022). Like in *C. difficile*, *B. subtilis* YabG is a sporulation-specific cysteine protease involved in the processing of several spore proteins during sporulation. Most target proteins of *B. subtilis* YabG (CotF, CotT, YeeK, YxeE, and SafA) are not conserved in *C. difficile* (Takamatsu, Imamura et al. 2000; Takamatsu, Kodama et al. 2000; Sebaihia et al. 2006). Additionally, the mechanism of target recognition and any additional targets remain unknown in *C. difficile*.

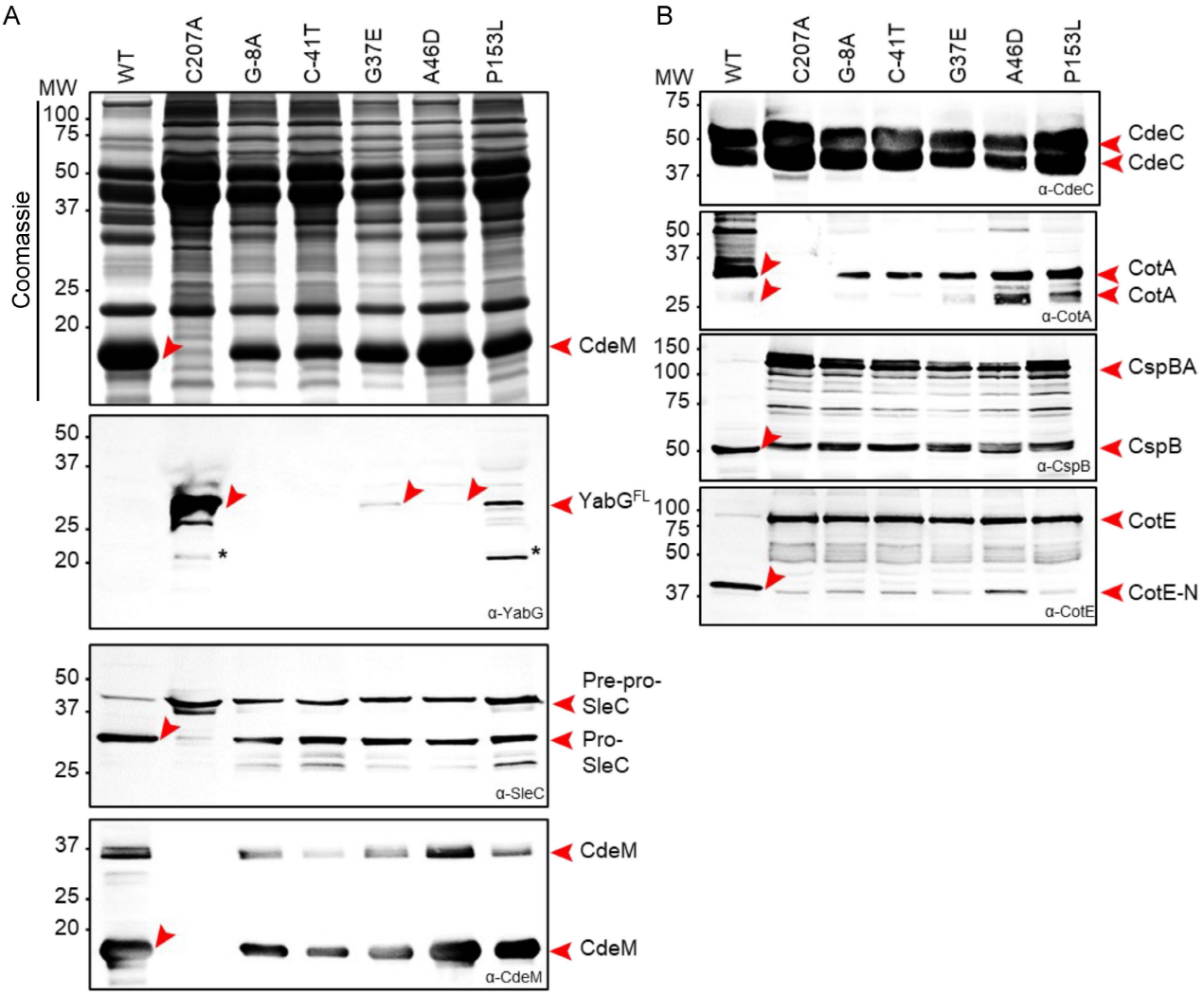

FIGURE 5 | *yabG* mutations affect the level and/or extractability of coat and exosporium proteins. Spores of the WT, $yabG_{C207A}$, and the various *yabG* point mutants, as shown, were purified, fractionated and the coat/exosporium and cortex/core proteins extracted. The proteins were resolved by 15% SDS-PAGE and the gels stained with Coomassie or subjected to immunoblot analysis with anti-YabG, anti-SleC, anti-CdeM (A), anti-CdeC, anti-CotA, anti-CspBA, and anti-CotE antibodies (B). The position of the proteins and their main forms, recognized by the different antibodies is indicated by the red arrowheads. The position of molecular weight (MW) markers (in kDa) is indicated on the left side of the panel.

In *C. difficile*, YabG processes CspBA to CspB and CspA and preproSleC to proSleC (Marini et al. 2023; Shrestha, Cochran, and Sorg 2019; Kevorkian, Shirley, and Shen 2016). However, in spores derived from a *C. difficile yabG* mutant, some CspB is present (Kevorkian, Shirley, and Shen 2016). This CspB form is due to either autoprocessing or another protease that is capable of processing CspBA (Kevorkian, Shirley, and Shen 2016; Marini et al. 2023; Shrestha, Cochran, and Sorg 2019). A previous study found a decrease in the abundance of SpoIVA in spores derived from a *C. difficile yabG* mutant, but the involvement of YabG in the incorporation of SpoIVA into mature spores is poorly understood (Kevorkian, Shirley, and Shen 2016). Because *C. difficile* YabG is the only protease with the ability to cleave preproSleC, and the preproSleC form is the only form incorporated into mature spores in *C. difficile yabG* mutants, preproSleC was used as our target to quantify the processing capabilities of YabG, $YabG_{C207A}$, $YabG_{A46D}$, $YabG_{P153L}$, and $YabG_{G37E}$ (Kevorkian, Shirley, and Shen 2016; Marini et al. 2023; Shrestha, Cochran, and Sorg 2019). We found that YabG is very efficient and processed ~50% of preproSleC to proSleC within 10 min and ~100% within 1 h of in vitro incubation (Figure 2A and Figure S1B). However, $YabG_{A46D}$ only processes 50% of preproSleC within 3 h of in vitro incubation (Figure 2C and Figure S1C). Interestingly, $YabG_{P153L}$ and $YabG_{G37E}$ did not show any activity at the times tested (Figure 2 and Figure S1). As only one target of YabG was tested, it is possible that these alleles are more active on other unidentified YabG targets. We consider this unlikely because of the defects in processing of numerous spore proteins observed by western blotting (Figure 5). CspBA is another YabG target, but some CspBA is processed and incorporated into mature spores of a *C. difficile* Δ*yabG* mutant strain. This suggests that another protease can cleave CspBA to CspB and CspA (Shrestha, Cochran, and Sorg 2019; Kevorkian, Shirley, and Shen 2016). Spores derived from the *C. difficile* R20291 *yabG::ermB* mutant strain only contained CspBA and not CspB and CspA (Shrestha, Cochran, and Sorg 2019) but our isogenic mutants (Figure 5B) contain some processed CspBA suggesting differences between the two *C. difficile* strains (*C. difficile*

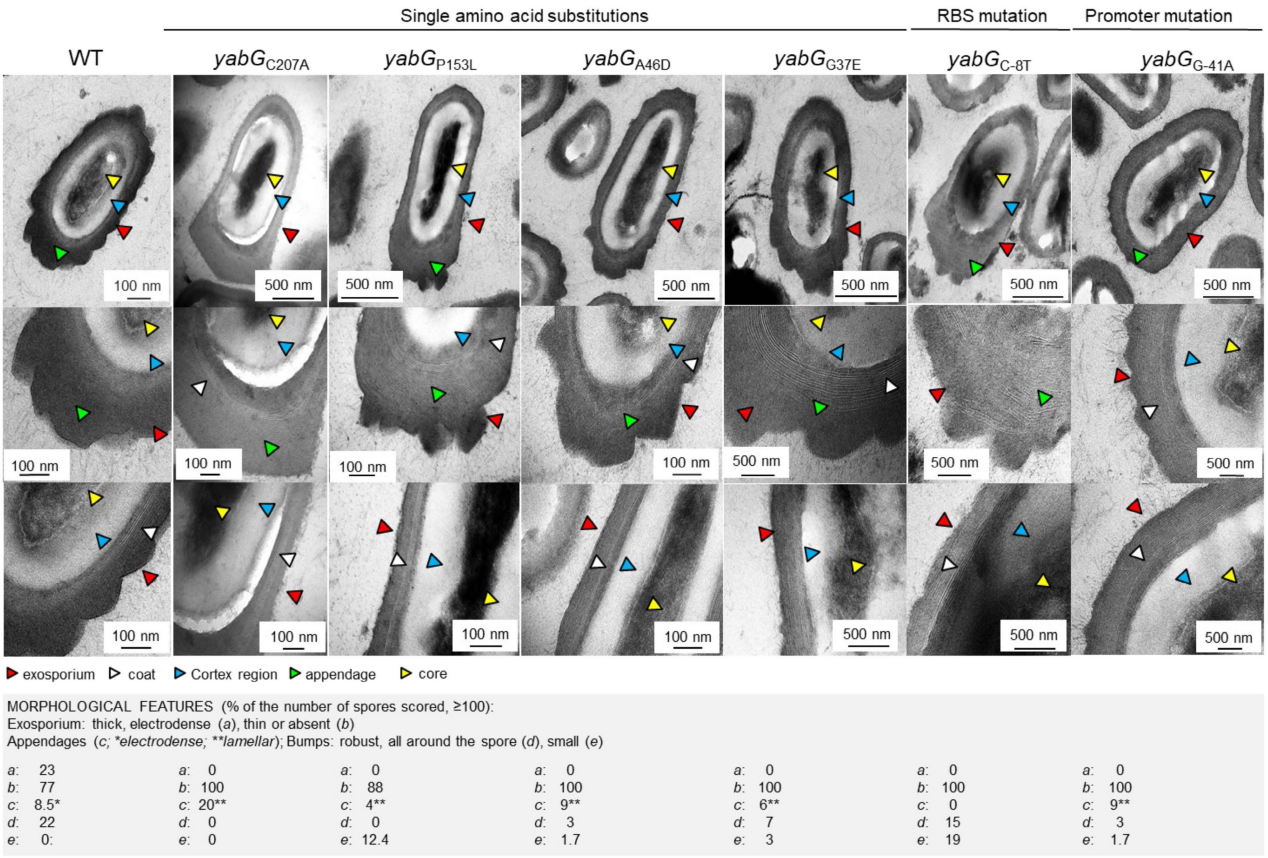

FIGURE 6 | Morphological alteration in spores of the yabG mutants. Gradient purified spores of the WT (630Δerm), yabG$_{C207A}$ and the indicated point mutants were analyzed by thin sectioning TEM. The arrowheads point to: the edge of the exosporium, red; the coat, white; the cortex, blue; the spore core, yellow; the electrodense regions within the spore appendage, green. The table refer to the percentage of spores (>100) in which the indicated feature is present; thick electrodense exosporium, a; thin or absent exosporium, b; electrodense lamellar appendage, c; bumps or robust appendage and all around the spore, d; and small bumpy appendage, e. Scale bars are indicated in the panels.

R20291 vs. *C. difficile* R20291 Δ*pyrE*) or because *yabG* is not produced in the *C. difficile* R20291 *yabG::ermB* mutant where as it is produced in *C. difficile* R20291 Δ*pyrE yabG*$_{C207A}$, but not catalytically active.

The processing site of YabG on preproSleC had previously been identified as R119. However, two other arginine residues are near R119, and we wanted to determine if YabG could also process at those sites (Shrestha, Cochran, and Sorg 2019). Interestingly, we found that upon mutation of preproSleC R119 to alanine, processing occurred at R115. In the preproSleC R119A/R115A mutant, processing occurred at R112. No processing was observed for the combined triple mutant, R119A/R115A/R112A. Interestingly, YabG does not cleave at R110 and in a predicted AlphaFold2 structure of preproSleC shows R119, R115, and R112 all reside within an exposed, unstructured loop, whereas R110 resides within a beta strand, mainly excluding it from processing (Figure 3B). It could also be the presence of P109 that excludes R110 from YabG processing.

All the spores derived from the *C. difficile* Δ*pyrE yabG* mutants germinated with TA only and did not require a co-germinant in order to germinate, unlike the parental *C. difficile* Δ*pyrE* strain (Figure 4). These results are consistent with previous findings. Interestingly, *C. difficile* Δ*pyrE yabG*$_{C207A}$ appears to germinate more slowly than the other mutants in TA only conditions. However, this may be due to the complete loss of YabG catalytic activity, resulting in a lack of processing of alterative targets (Shrestha, Cochran, and Sorg 2019).

Spores derived from the *C. difficile* Δ*yabG* and *C. difficile yabG*$_{C207A}$ strains incorporate less CotA and CdeM (Figure 5A,B) (Marini et al. 2023). CotA is a component of the spore coat and is required for assembly of the outer surface layers of the spore (Permpoonpattana et al. 2011, 2013). CdeM is a component of the exosporium (Calderón-Romero et al. 2018). Upon investigation of *cdeC* and *cdeM* transcript levels of *C. difficile* Δ*yabG* sporulating cells, their levels were lower compared to wild type, suggesting YabG was regulating their transcription, though the mechanism by which this occurs remains unknown (Marini et al. 2023). It has also been observed in *Clostridium botulinum* that a disruption of *yabG* by a prophage-like DNA insertion (*yin* element) resulted in early onset sporulation compared to strains lacking that element (Douillard et al. 2023). These findings highlight that YabG in other organisms may be playing a role in sporulation regulation. To investigate if the C. *difficile yabG* alleles also affect spore cortex/coat/exosporium proteins, western blots were performed against CdeM, CdeC, CotA, CotE, CspBA, preproSleC, and YabG. CdeM was less abundant or less extractable from the purified spores of *C. difficile*

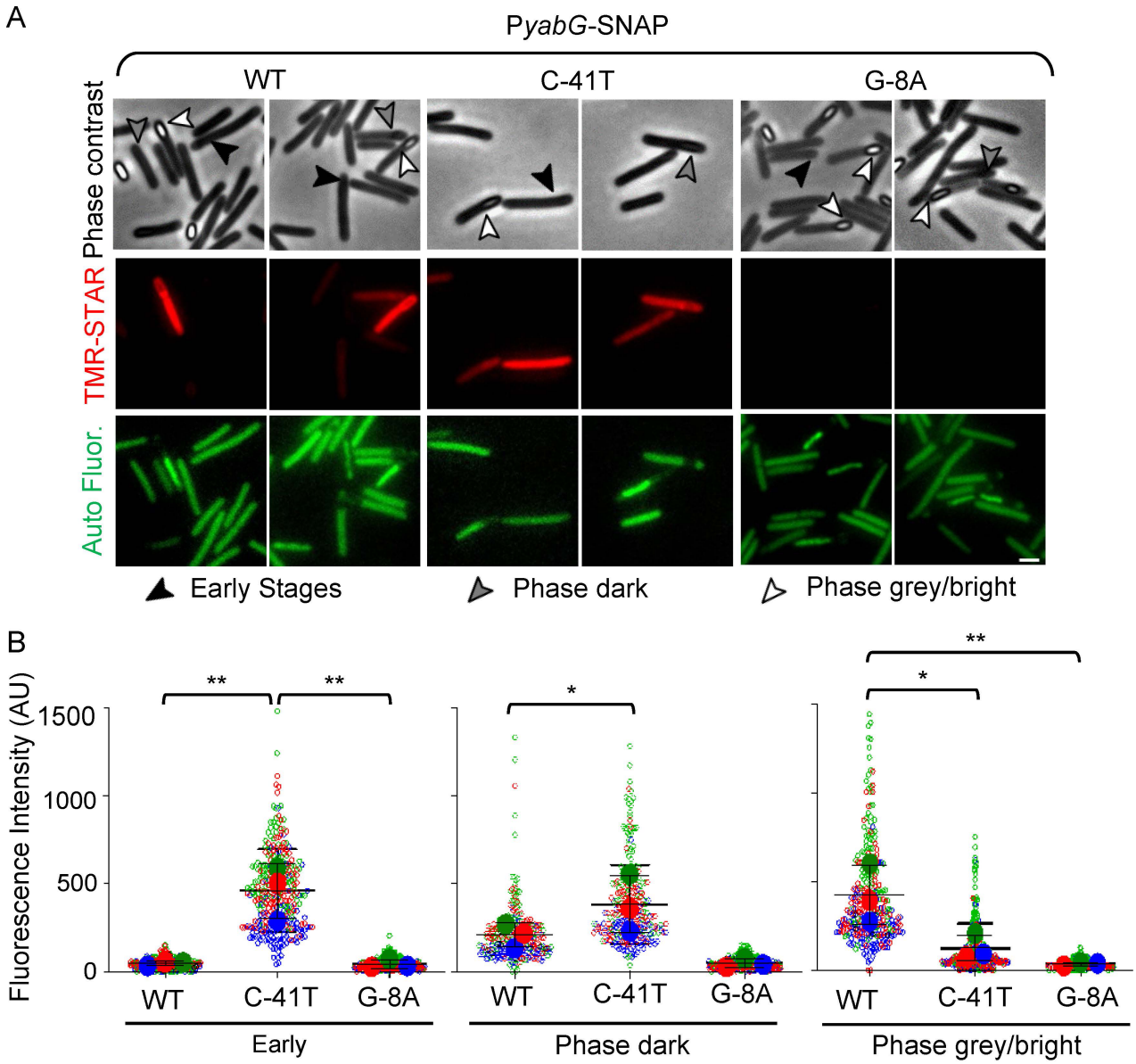

FIGURE 7 | Single cell analysis of P*yabG* expression. (A) *C. difficile* sporulating cells carrying fusions of the WT *yabG* promoter or alleles with the G-8A or C-41 T mutations fused to the *SNAP*^{Cd} reporter in an otherwise WT background (630Δ*erm*) were collected after 20 h of growth on 70:30 agar plates. The cells were stained with the SNAP substrate TMR-Star and examined by phase contrast (top panels) and fluorescence microscopy (middle panel, SNAP^{Cd} signal; bottom panels, autofluorescence). The black arrowheads show cells at early stages of sporulation, with no visible signs of a forespore; the gray arrowheads show sporangia of phase dark forespores and the white arrowheads indicate sporangia of phase gray or phase bright forespores. Scale bar, 1 μm. (B) Intensity of the fluorescence signal per cell for the P$_{yabG}$-*SNAP*^{Cd} fusions described in (A) in cells at early stages of sporulation or in sporangia of phase dark or phase gray/phase bright forespores. Fluorescence intensity is shown in arbitrary units (AU). The data from three independent experiments was represented using SuperPlots, with each color corresponding to a replicate (Lord et al. 2020). Statistical analysis was carried out using the ordinary one-way ANOVA and Tukey's test. Asterisks correspond to p values of $p < 0.05$ (*) or $p < 0.01$ (**).

Δ*pyrE yabG*$_{C\text{-}41T}$ (Figure 5A). In *C. difficile* Δ*pyrE yabG*$_{C\text{-}41T}$ expression of the reporter is even higher than in the wild type (Figure 7B), which could potentially be due to earlier expression of *yabG* interfering with transcription of *cdeM* and *cotA* and/or assembly of the proteins (Figure 5). Interestingly, the levels/extractability of CdeM and CotA, were higher in *C. difficile* Δ*pyrE yabG*$_{A46D}$ and *C. difficile* Δ*pyrE yabG*$_{P153L}$ spores, as compared to *C. difficile* Δ*pyrE yabG*$_{G37E}$ spores (Figure 5A,B). One possibility is that the *yabG*$_{A46D}$ and *yabG*$_{P153L}$ alleles are more efficient than the *yabG*$_{G37A}$ allele at promoting *cdeM* and *cotA* transcription. Processing of preproSleC, CspBA and CotE is incomplete (Figure 5A,B), and we do not know the location or timing of these events. Because proSleC and CspB and CspA are found in the cortex, we hypothesize that they are processed in the cytoplasm before being transported to the cortex (Baloh, Nerber, and Sorg 2022).

YabG was not detected in the promoter mutant *C. difficile* Δ*pyrE yabG*$_{C\text{-}41T}$ or the RBS mutant *C. difficile* Δ*pyrE yabG*$_{G\text{-}8A}$, similar to wild type. This is most likely due to its auto-proteolytic activity, however the lack of YabG in *C. difficile* Δ*pyrE yabG*$_{G\text{-}8A}$ is likely due to loss of expression (Figures 5A and 7B) (Marini

et al. 2023). In all *yabG* mutants with a single amino acid substitution (G37A, A46D, and P153L), YabG was detected in the spore extracts, but at levels lower than the catalytically inactive $YabG_{C207A}$ allele. This suggests that these variants are less active than the WT protein (Figure 5A). Consistent with the lower activity of $YabG_{P153L}$, autoprocessing and processing of prepro-SleC, CspBA, and CotE was diminished relative to *C. difficile* $yabG_{G37E}$ and *C. difficile* $yabG_{A46D}$ (Figure 5A,B).

C. difficile Δ*pyrE* $yabG_{A46D}$ showed the lowest amount of YabG in spore extracts of the three single amino acid substitution mutants. This is consistent with $YabG_{A46D}$ showing activity against purified preproSleC in vitro (Figures 2C and 5A). Reduced activity of YabG can result from single amino acid substitutions in different parts of the protein (A46D and G37E in the SH3 domain; P153L in the CheY-like, catalytic domain). Together this suggests that the different alleles have various levels of catalytic activity.

The main morphological changes in *C. difficile* Δ*yabG* or *C. difficile* $yabG_{C207A}$ spores include a loose connection between the cortex and coat layers, a thin outermost electron dense layer (thought to be part of the exosporium), and a lack of electron density in the appendage region, which reveals an underlying pattern of lamellae (Marini et al. 2023). The thinner outer layer and the lack of electron density of the spore appendage is thought to be caused by the absence of CdeM, as it is not expressed in *yabG* mutants. Accordingly, the electron density of the appendage is restored when *cdeM* is expressed from the *yabG*-independent *cotE* promoter (Marini et al. 2023). *C. difficile* *yabG* mutants, were originally studies in *C. difficile* 630Δ*erm*, however, we used *C. difficile* R20291 Δ*pyrE* as a parental strain (Marini et al. 2023). A striking difference between spores of the two strains is that the outermost electron dense spore layer is much thicker in R20291 spores and presents bumps that protrude from the entire surface of the spore (Figure 6, wild type spores). Apart from the *C. difficile* $yabG_{C207A}$ mutant, there were no overt signs of an impaired cortex/coat connection in the point mutation strains, suggesting that a lower level of YabG activity is sufficient to prevent this phenotype (Figure 6).

It remains unknown how YabG recognizes its targets in any organism. In *B. subtilis*, YabG processes coat proteins, however only SpoIVA has an orthologue in *C. difficile* (Kuwana et al. 2006; Takamatsu, Imamura et al. 2000; Takamatsu, Kodama et al. 2000; Yamazawa et al. 2022). Moreover, despite universal conservation of the protein in spore forming bacteria, the absence of conserved substrates is intriguing. Future work needs to be done to identify YabG substrates and reveal any conserved features that may help to identify substrates in other non-model, spore forming organisms.

4 | Experimental Procedures

4.1 | Bacterial Growth Conditions

All bacterial strains are listed in Table S2. *C. difficile* strains were derivatives of 630Δ*erm* or R20291 grown in a Coy anaerobic chamber at 37°C, 3–4% H_2, 5% CO_2, and balanced N_2 on either brain heart infusion (BHI) medium (Difco) supplemented with 0.1% L-cysteine and BHI supplemented with 5 g/L yeast extract and 0.1% L-cysteine (BHIS) or 70:30 media as indicated. When necessary, media was supplemented with thiamphenicol (10–15 μg/mL), kanamycin (50 μg/mL), D-cycloserine (250 μg/mL), tetracycline (5 μg/mL), uracil (2 μg/mL), theophylline (2 g/L), cefoxitin (25 μg/mL), and/or taurocholate (TA) (0.1%). Defined minimal media for *C. difficile* (CDMM) supplemented with 5-fluoroorotic acid (FOA; 2 mg/mL) and uracil (5 μg/mL) was used for the selection of Δ*pyrE* mutants. *E. coli* strains were grown at 37°C on LB medium supplemented with chloramphenicol (20 μg/mL) and or ampicillin (100 μg/mL) for plasmid maintenance. *E. coli* BL21 (DE3) was grown in 2x tryptone yeast (2XTY), medium supplemented with chloramphenicol (20 μg/mL) and/or ampicillin (100 μg/mL) for plasmid maintenance and used for recombinant protein expression.

4.2 | Plasmid Constructions

The oligonucleotide primers used in this work are listed in Table S1. Plasmids pMS17, pMS43, pMS44, and pMS45 were made from pMTL-YN4 as follows. PMTL-YN4 was digested with MluI/XhoI and purified by gel electrophoresis, extracted, then assembled with their respective regions of homology via Gibson assembly (Gibson et al. 2009). Regions of pMS17 homology were amplified from *C. difficile* R20291 with primers 5′ yabG C207A pMTL-YN4, 3′ yabG C207A upstream, 5′ yabG C207A downstream, and 3′ yabG C207A pMTL-YN4. Region of pMS43 homology were amplified from *C. difficile* mutant 20C using primer pairs 5′ yabG A46D_up/3′ yabG A46D_up, and 5′ yabG A46D_down/and 3′ yabG A46D_down. Regions of pMS44 were amplified from *C. difficile* mutant 30A using primer pairs 5′ yabG P153L_up/3′ yabG P153L_up and 5′ yabG P153L_down/3′ yabG P153L_down, respectively. Regions of pMS45 homology were amplified from *C. difficile* mutant 30C using primer pairs 5′ yabG G37E_up/3′ yabG G37D_up and 5′ yabG G37E_down/3′ yabG G37E_down. Plasmids pJB86 and pJB87 were made from pJB81 as follows. pJB81 was digested by NotI/XhoI and purified by gel electrophoresis, extracted, then assembled with their respective regions of homology via Gibson assembly. Regions of homology for pJB86 were amplified with primers 5′ prom_C-8T_up/3′ prom_C-8T_up and 5′ prom_C-8T_down/3′ prom_C-8T_down, while those for pJB87 were amplified with primers 5′ yabG_G-41A_up/3′ yabG_G-41A_up and 5′ yabG_G-41A_down/3′ yabG_G-41A_down. After Gibson assembly and transformation into *E. coli* DH5α (Hanahan 1983), colonies were re-streaked and tested via PCR for correct assembly, followed by whole plasmid sequencing.

Plasmids pMS48, pMS49, pMS50, pMS51, pMS59, and pMS60 were made from pET22b as follows. pET22b was digested with NdeI/XhoI and purified by gel electrophoresis, extracted, then assembled with their respective regions of homology via Gibson assembly. Regions of pMS48 homology were amplified from *C. difficile* R20291 using primer pairs 5′ pET22b_yabG_up/3′ yabG A46D_up and 3′ yabG A46D_up/3′ pET22b_yabG_down. Regions of pMS49 homology were amplified from *C. difficile* mutant 30A using primer pairs primer pairs 5′ pET22b_yabG_up and 3′ pET22b_yabG_down. Regions of pMS50 were amplified from *C. difficile* mutant 30C using primer pairs 5′ pET22b_yabG_up and 3′ pET22b_yabG_down. Regions of

pMS51 were amplified from *C. difficile* MRS05 using primer pairs 5′ pET22b_yabG_up and 3′ pET22b_yabG_down. Regions of pMS59 were amplified from *C. difficile* R20291 using primer pairs 5′ pET22b preproSleC/3′ pET22b R112A and 5′ pET22b R112A and 3′ pET_SleC. Regions of pMS60 were amplified from *C. difficile* R20291 using primer pairs 5′ pET22b preproSleC/3′ pET22b R112A/R115A and 5′ pET22b R112A/R115A/3′ pET_SleC. After Gibson assembly and transformation into *E. coli* DH5α, colonies were re-streaked and tested via PCR for correct assembly, followed by whole plasmid sequencing.

Plasmids pAC57, pAC58, and pAC59 were made from pET22b as follows. pET22b was digested with NdeI/BamHI and purified by gel electrophoresis, extracted, then assembled with their respective regions of homology via Gibson assembly. Regions of pAC57 were amplified from *C. difficile* R20291 using primers SleC 119A_Fp/pet22b_yabg_SleC6his_Rp and pet22b_SleC_Fp/SleC R119A_Rp. Regions of pAC58 were amplified from *C. difficile* R20291 using primer pairs SleC 119115112A_Fp/pet22b_yabg_SleC6his_Rp and pet22b_SleC_Fp/SleC 119115112A_Rp. Regions of pAC59 were amplified from *C. difficile* R20291 using primer pairs SleC 119115A_Fp/pet22b_yabg_SleC6his_Rp and pet22b_SleC_Fp/SleC 119115A_Rp. After Gibson assembly and transformation into *E. coli* DH5α, colonies were re-streaked and tested via PCR for correct assembly, followed by whole plasmid sequencing using Oxford Nanopore Technology by Plasmidsaurus Inc. (Eugene, OR).

4.3 | Conjugations

The plasmids pMS17, pMS43, pMS44, and pMS45 were conjugated separately into *C. difficile* Δ*pyrE* for Δ*pyrE*-mediated allele-coupled exchange (ACE) (Ng et al. 2013) using *E. coli* HB101 pRK24 as a conjugal donor. The plasmid was transformed into *E. coli* HB101 pRK24 and plated on LB-agar supplemented with chloramphenicol and ampicillin and grown overnight. An overnight culture of *E. coli* HB101 was grown in 5 mL of BHIS supplemented with chloramphenicol and ampicillin, *C. difficile* Δ*pyrE* was grown in 5 mL of BHIS. Five hundred microliter of the *E. coli* overnight culture was pelleted, supernatant discarded, and transferred into the anaerobic chamber. One milliliter of overnight *C. difficile* Δ*pyrE* culture was heated for 5 min at 52°C and let rest for 2 min (Kirk and Fagan 2016). The *E. coli* was resuspended with 1 mL of the heat shocked *C. difficile* Δ*pyrE*. Four to five spots of 50 μL of mixed culture were plated on BHI and incubated for approximately 24 h. Growth was resuspended in 1 mL of BHIS and plated on BHIS supplemented with thiamphenicol, uracil, kanamycin, and D-cycloserine, for selection (BHIS TUCK). The resulting transconjugant colonies were streaked for tetracycline sensitivity and thiamphenicol resistance and confirmed by PCR.

4.4 | ΔpyrE-Mediated Allelic Exchange

C. difficile strains MRS04, MRS05, MRS06, and MRS07 were made as previously described (Ng et al. 2013) from parental strain KNM05 (McAllister et al. 2017) with plasmids, pMS43, pMS17, pMS45, and pMS44, respectively. Briefly, transconjugants were passaged on BHIS supplemented with thiamphenicol, uracil, D-cycloserine, and kanamycin. Integrants were passaged onto CDMM + FOA + uracil. Colonies were passaged onto BHIS and BHIS supplemented with thiamphenicol to screen for plasmid loss. Loss of plasmid was confirmed by PCR and whole genome re-sequencing was performed to confirm genotype.

4.5 | Theophylline-Mediated Allelic Exchange

C. difficile strains JNB25 and JNB26 were made as previously described (Brehm and Sorg 2024) from parental strain KNM05 with plasmids pJB87 and pJB86, respectively. Briefly, the plasmids were introduced into KNM05 via *E. coli* HB101 pRK24 conjugation and confirmed by PCR. Transconjugants were plated on BHIS Tm plates, where plasmid integration was screened by colony size. Colonies that contained the integrated plasmid were isolated and plated on BHIS containing 2 g/L theophylline to encourage plasmid excision. Colonies were isolated and tested for their respective mutations by PCR amplification and sequencing, followed by whole genome sequencing of the completed strains. Whole genome sequencing was performed on strains and sent for Illumina sequencing at SeqCoast Genomics LLC (Portsmouth, NH) and raw sequence reads are uploaded to the Sequence Read Archive under BioProject ID: PRJNA1112411.

4.6 | SNAP^{Cd} Fusions

To construct the P*yabG* transcriptional fusions to the SNAP^{Cd} reporter, the promoter regions of *yabG* were PCR-amplified using as the template genomic DNA of *C. difficile* R20291 Δ*pyrE* 31D (strain 4049030, bearing the C-8T mutation), *C. difficile* R20291 Δ*pyrE* 27E (strain 4049063, with the G-41A mutation) or *C. difficile* R20291Δ*pyrE* (lab strain AHCD774, *yabG*^{WT}). The primer pairs used were PyabG-EcoRI-Fw and C8T-SNAP-SOE-Rev for the first strain and PyabG-EcoRI-Fw and YabG-978-SOE-Rev for the last two strains. The PCR reactions produced fragments of 271 bp. The SNAP^{Cd} gene was PCR amplified from pFT47 (Pereira et al. 2013) using primers SNAP-Fw and SNAPCd-*HindIII*-Rev to produce a fragment with 558 bp. The two fragments were joined by PCR using primers PyabG-EcoRI-Fw and SNAPCd-*HindIII*-Rev. This produced fragments of 809 bp which were cleaved using EcoRI and HindIII and inserted between the same sites of pMTL84121. This originated plasmids pCO39 (P*yabG*-SNAP^{Cd}), pCO40 (P*yabG*^{C8T}-SNAP^{Cd}), and pCO41 (P*yabG*^{G42A}-SNAP^{Cd}). These plasmids were transformed into *E. coli* HB101 (RP4) originating strains AHEC1588 (pCO39), AHEC1589 (pCO40), and AHEC1590 (pCO41) and then transferred to *C. difficile* 630Δ*erm pyrE*$^{+}$ (AHCD1190) by conjugation to produce strains AHCD1842, AHCD1843, and AHCD1844, respectively. All primers are listed in Table S1. All strains and plasmids are listed in Table S2.

4.7 | Germination Assay

Germination was monitored using a Spectramax M3 plate reader (Molecular Devices, Sunnyvale, CA) (Shrestha, Lockless, and Sorg 2017; Bhattacharjee and Sorg 2018; Shrestha and Sorg 2018, 2019; Shrestha, Cochran, and Sorg 2019). $OD_{600} = 100$ spores were heat activated for 30 min at 65°C. Five microliter of spores was added to 95 μL of germination buffer containing

50 mM HEPES alone, or HEPES supplemented with 10 mM TA or with 10 mM TA and 30 mM glycine in a 100 μL total volume. The OD_{600} was monitored for 1 h at 37°C.

4.8 | SleC Expression and Purification

Plasmid pKS08 was transformed into *E. coli Rosetta* BL21 (DE3) and incubated overnight at 37°C on LB-agar supplemented with chloramphenicol and ampicillin. The plate was scraped into 1 mL of LB and used to inoculate 1 L of 2XTY supplemented with chloramphenicol and ampicillin in baffled flasks ($OD_{600} = 0.01$). The culture was incubated at 37°C at 190 rpm until the OD_{600} was between 0.6 and 0.8, at which point the culture was induced with 250 μM IPTG and incubated for 16 h at 16°C and 130 rpm. Cultures were pelleted at 6370×g for 15 min at 4°C. Supernatant was discarded and pellets were stored at −80°C until use. One liter of cells was resuspended in 25 mL of 300 mM NaCl, 50 mM Tris–HCl, 15 mM imidazole (pH 7.5) and 0.03 mM PMSF. Each 25 mL of cells was supplemented with lysozyme and DNase I and was rocked for 30 min at 4°C prior to sonication on ice at 27% amplitude for 20 min. Samples were then centrifuged at 25,900×*g* for 30 min at 4°C and the supernatant was combined with 1 mL of Ni-NTA Agarose beads. Samples were rocked overnight at 4°C. Beads were washed twice with 300 mM NaCl, 50 mM Tris–HCl, 30 mM imidazole (pH 7.5). Beads were washed once with 300 mM NaCl, 50 mM Tris–HCl, 15 mM imidazole (pH 7.5) and then eluted with the same buffer but supplemented with 500 mM imidazole. Samples were concentrated using a 10 kDA molecular weight cut off centrifugal device. The protein was further purified by size exclusion chromatography using a Cytiva ÄKTA Pure system (Marlborough, MA) on a Superdex 200 increase 10/300 GL column and concentrated again. Protein was diluted to 2.5 mg/mL, aliquoted, flash frozen in a dry ice–ethanol bath, and stored at −80°C until use.

4.9 | YabG In Vitro Lysate Preparation

Plasmids containing wild type (pAC28), mutant (pMS48, pMS49, pMS50, and pMS51) *yabG*, or an empty pET22b vector were transformed into *E. coli Rosetta* BL21 (DE3), and incubated overnight at 37°C on LB-agar supplemented with chloramphenicol and ampicillin. The plate was scraped into 1 mL of LB and used to inoculate 50 mL of LB supplemented with chloramphenicol and ampicillin in 250 mL flasks, so the starting culture OD_{600} was at 0.01. The culture was incubated at 37°C at 170 rpm until the OD_{600} was between 0.6 and 0.7. The culture was induced with 250 μM IPTG and incubated for 1 h at 37°C. YabG cultures were pelleted by centrifugation at 4415×*g*, for 15 min at 4°C. The supernatant was discarded, and cells were resuspended in 4 mL of 300 mM NaCl, 50 mM Tris–HCl (pH 7.5) before sonication on ice at 27% amplitude for 20 min. Bacterial lysate was immediately used in the SleC processing assay.

4.10 | SleC Processing Assay

The expression difference between wild type *yabG* and of each *yabG* alleles was determined through immunoblotting with an anti-His antibody (Invitrogen). The percent wildtype is as follows; $yabG_{G37E}$ 19.1% (5.24× lysate added to assays), $yabG_{A46D}$ 21.9% (4.57× lysate added to assays), $yabG_{P153L}$ 32.1% (3.12× lysate added to assays), and $yabG_{C207A}$ 31.2% (3.12× lysate added to assays).

Recombinantly expressed and purified preproSleC from *E. coli* was incubated with the indicated recombinantly expressed *yabG* allele lysate. Incubations were conducted at 37°C for 1, 5, 10, 15, 20, 25, 30 min, 1, 2, or 3 h. The reactions occurred in 25 μL total volume [56 μg preproSleC present in 22.5 μL + 2.5 μL of the indicated *yabG* allele or buffer 300 mM NaCl, 50 mM Tris–HCl (pH 7.5)]. As a control, purified preproSleC was added to buffer alone. Samples were denatured at 95°C for 20 min, diluted with 1× Nu-PAGE sample buffer, and stored at 4°C until use.

42 ng of purified SleC from the SleC processing assays were separated by 12% sodium dodecyl sulfate (SDS)-PAGE. Protein was then transferred onto low-fluorescence polyvinylidene difluoride membrane (PVDF) using the Hoefer TE 62 tank transfer system at 1.0 A for 1 h. The membranes were blocked in 5% skim milk in Tris-buffered saline with 0.1% Tween-20 (TBST) rocking overnight at 4°C. The membranes were incubated with anti-SleC antibody for 1 h in 5% skim milk in TBST and washed three times with TBST. For the secondary antibody, LI-COR IRDye 680RD goat anti-rabbit antibody was used to label the membranes for 1 h in 5% skim milk in TBST in the dark. The membranes were washed three times, in the dark, with TBST. Blots were imaged wet on the Odyssey CLx and the Odyssey M imaging systems (Li-COR, Lincoln, NE) using the 700–800 nm channels. The fluorescent bands were visualized and analyzed using ImageStudio software version 5.2 or LI-COR Acquisition software version 1.2 and analyzed with Empiria Studio version 2.3 (LI-COR Biosciences).

4.11 | Edman Sequencing

Plasmids pKS08, pAC57, pAC59, pAC58, pMS60, and pMS59 were induced and protein was purified the same as described above. Purified preproSleC, $preproSleC_{R119A}$, $preproSleC_{R119A/R115A}$, $preproSleC_{R119A/R115A/R112A}$, $preproSleC_{R115A/R112A}$, and $preproSleC_{R112A}$ were incubated with *E. coli* lysate expressing wild type *yabG* for 3 h. The preproSleC processing assays were separated on a 12% SDS-PAGE and transferred to PVDF membrane using the BIO-RAD Trans-Blot Turbo Transfer system at 25 V, 1.0 A for 30 min. The membrane was thoroughly washed under dH_2O for ~10 min to remove residual glycine. The membrane was stained with Coomassie Brilliant Blue for 20 min (50% MeOH, 10% acetic acid, 40% dH_2O, and 0.05% Coomassie). The membrane was destained (50% MeOH, 10% acetic acid, and 40% dH_2O). The proSleC band was excised from the membrane using a fresh razor blade. The band was sent for Edman sequencing of the first five amino acids at The Protein Facility at Iowa State University.

4.12 | Spore Purification

Spores were purified as described previously (Nerber, Baloh, and Sorg 2023; Aguirre, Adegbite, and Sorg 2022; Baloh, Nerber, and Sorg 2022; Baloh and Sorg 2021; Shrestha, Cochran, and Sorg 2019; Shrestha and Sorg 2018, 2019; Bhattacharjee et al. 2016). Briefly,

cultures were plated on BHIS media (BHI with 5% yeast extract) and incubated for 4–5 days. Cells from each plate were scraped into 1 mL of 18 Ω H_2O and incubated overnight at 4°C. Cells were washed with 18 Ω H_2O approximately five times and four tubes were combined into one tube of 1 mL. The washed spores were then layered on top of 9 mL of 50% sucrose and centrifuged at 4000×*g* for 20 min at 4°C. The supernatant was discarded, and the spores were washed approximately five more times with 18 Ω H_2O and stored at 4°C until use.

4.13 | Spore Production, Purification and Extraction of Spore Proteins

Spores were purified from 70:30 agar plates after 20 h of growth using a step gradient of Gastrografin (Bayer) as described (Marini et al. 2023). The spore titer in the final suspension was estimated by measuring the OD_{580}. The sediment was resuspended in 5 mL of BHI centrifuged (4000×*g*, for 5 min at 4°C) and the sediment resuspended in 1 mL of extraction buffer [0.125 mM Tris (hydroxymethyl) aminomethane hydrochloric acid (Tris–HCl), 5% β-mercaptoethanol, 2% SDS, 0.025% bromophenol blue, 0.5 mM dithiothreitol (DTT), 5% glycerol, pH 6.8] and the suspension boiled for 8 min (Marini et al. 2023).

4.14 | Transmission Electron Microscopy

Thin sectioning TEM of density gradient-purified *C. difficile* spores, prepared following 20 h of growth on 70:30 plates (above) was as described previously (Marini et al. 2023).

4.15 | SDS-PAGE and Immunoblot Analysis of Spore Extracts

Proteins extracted from whole spores were resolved by SDS-PAGE (15% gels) and visualized by Coomassie brilliant blue R-250 staining. Gels run in parallel were subject to immunoblot analysis using the following antibodies at the indicated dilutions: anti-YabG (1:1000), anti-CdeC (1:500), anti-CdeM (1:15000), anti-CotA (1:1000), anti-CspB, anti-CspC, and anti-SleC (1:3000), anti-GPR (1:10000), and anti-SNAP-tag at 1:1000. A rabbit secondary antibody conjugated to horseradish peroxidase (Sigma) was used at a dilution of 1:5000; while anti-mouse IgG (whole molecule)-peroxidase (Sigma), at a dilution of 1:2000. The immunoblots were developed with Super Signal Pico Plus Chemiluminescent Substrate (Thermo Scientific).

4.16 | $SNAP^{Cd}$ Labeling, Phase Contrast, Fluorescence Microscopy, and Image Analysis

For SNAP labeling, cells were withdrawn from sporulating cultures after 20 h of growth on 70:30 medium (Putnam et al. 2013); the samples were mixed for 30 min in the dark with the TMR-Star substrate (New England Biolabs) at a final concentration of 250 nM (Pereira et al. 2013). Cells were collected by centrifugation (4000×*g* for 5 min at room temperature), washed four times with 1 mL of phosphate-buffered saline (PBS; 137 mM NaCl, 10 mM Phosphate, 2.7 mM KCl, pH 7.4), and resuspended in 0.5 mL of PBS. For phase contrast and fluorescence microscopy, cells were mounted on 1.7% agarose-coated glass slides and observed on a Leica DM6000B microscope equipped with a phase contrast Uplan F1 100× objective and captured with a CCD Andor Ixon camera (Andor Technologies). Images were acquired and analyzed using the Metamorph software suite (version 5.8; Universal Imaging) and adjusted and cropped using ImageJ.

4.17 | Statistical Analysis

All processing assays and germination assays were performed in at least biological triplicate and the data represents the averages from the data sets. Error bars represent the standard error of the mean. A one-way ANOVA Šídák's multiple comparisons test was used to compare the quantified protein amounts.

Author Contributions

Morgan S. Osborne: conceptualization, methodology, validation, formal analysis, data curation, writing – original draft, writing – review and editing. **Joshua N. Brehm:** methodology, validation, formal analysis, writing – review and editing. **Carmen Olivença:** methodology, data curation, writing – review and editing. **Alicia M. Cochran:** methodology, data curation. **Mónica Serrano:** formal analysis, writing – review and editing. **Adriano O. Henriques:** conceptualization, methodology, writing – review and editing. **Joseph A. Sorg:** conceptualization, methodology, writing – original draft, writing – review and editing, supervision, project administration, funding acquisition.

Acknowledgments

We thank members of the Sorg laboratory for critical comments during the preparation of this manuscript. We also thank Joel Nott at The Protein Facility of Iowa State University for performing the Edman sequencing. This project was supported by awards 5R01AI116895 and 5R01AI172043 to J.A.S. from the National Institute of Allergy and Infectious Diseases. The content is solely the responsibility of the authors and does not necessarily represent the official views of the NIAID. The funders had no role in study design, data collection and interpretation, or the decision to submit the work for publication.

Conflicts of Interest

The authors declare no conflicts of interest.

Data Availability Statement

The data that support the findings of this study are available from the corresponding author upon reasonable request.

References

Adams, C. M., B. E. Eckenroth, E. E. Putnam, S. Doublié, and A. Shen. 2013. "Structural and Functional Analysis of the CspB Protease Required for *Clostridium* Spore Germination." *PLoS Pathogens* 9: e1003165.

Aguirre, A. M., A. O. Adegbite, and J. A. Sorg. 2022. "*Clostridioides difficile* Bile Salt Hydrolase Activity Has Substrate Specificity and Affects Biofilm Formation." *npj Biofilms and Microbiomes* 8: 94.

Baloh, M., H. N. Nerber, and J. A. Sorg. 2022. "Imaging *Clostridioides difficile* Spore Germination and Germination Proteins." *Journal of Bacteriology* 204: e0021022.

Baloh, M., and J. A. Sorg. 2021. "*Clostridioides difficile* SpoVAD and SpoVAE Interact and Are Required for Dipicolinic Acid Uptake Into Spores." *Journal of Bacteriology* 203: e0039421.

Bhattacharjee, D., M. B. Francis, X. Ding, K. N. McAllister, R. Shrestha, and J. A. Sorg. 2016. "Reexamining the Germination Phenotypes of Several *Clostridium difficile* Strains Suggests Another Role for the CspC Germinant Receptor." *Journal of Bacteriology* 198: 777–786.

Bhattacharjee, D., K. N. McAllister, and J. A. Sorg. 2016. "Germinants and Their Receptors in Clostridia." *Journal of Bacteriology* 198: 2767–2775.

Bhattacharjee, D., and J. A. Sorg. 2018. "Conservation of the "Outside-In" Germination Pathway in *Paraclostridium bifermentans*." *Frontiers in Microbiology* 9: 2487. https://doi.org/10.3389/fmicb.2018.02487.

Brehm, J. N., and J. A. Sorg. 2024. "Theophylline-Based Control of repA on a *Clostridioides difficile* Plasmid for Use in Allelic Exchange." *Anaerobe* 88: 102858.

Buffie, C. G., V. Bucci, R. R. Stein, et al. 2015. "Precision microbiome reconstitution restores bile acid mediated resistance to *Clostridium difficile*." *Nature* 517: 205–208.

Calderón-Romero, P., P. Castro-Córdova, R. Reyes-Ramírez, et al. 2018. "*Clostridium difficile* Exosporium Cysteine-Rich Proteins Are Essential for the Morphogenesis of the Exosporium Layer, Spore Resistance, and Affect *C. difficile* Pathogenesis." *PLoS Pathogens* 14: e1007199.

Deakin, L. J., S. Clare, R. P. Fagan, et al. 2012. "The *Clostridium difficile spo0A* Gene Is a Persistence and Transmission Factor." *Infection and Immunity* 80: 2704–2711.

Di Bella, S., G. Sanson, J. Monticelli, et al. 2024. "*Clostridioides difficile* Infection: History, Epidemiology, Risk Factors, Prevention, Clinical Manifestations, Treatment, and Future Options." *Clinical Microbiology Reviews* 37, no. 2: e0013523. https://doi.org/10.1128/cmr.00135-23.

Douillard, F. P., I. M. Portinha, Y. Derman, et al. 2023. "A Novel Prophage-Like Insertion Element Within yabG Triggers Early Entry Into Sporulation in *Clostridium botulinum*." *Viruses* 15, no. 12: 2431. https://doi.org/10.3390/v15122431.

Fimlaid, K. A., J. P. Bond, K. C. Schutz, et al. 2013. "Global Analysis of the Sporulation Pathway of *Clostridium difficile*." *PLoS Genetics* 9: e1003660.

Francis, M. B., C. A. Allen, R. Shrestha, and J. A. Sorg. 2013. "Bile Acid Recognition by the *Clostridium difficile* Germinant Receptor, CspC, Is Important for Establishing Infection." *PLoS Pathogens* 9: e1003356.

Francis, M. B., C. A. Allen, and J. A. Sorg. 2015. "Spore Cortex Hydrolysis Precedes Dipicolinic Acid Release During *Clostridium difficile* Spore Germination." *Journal of Bacteriology* 197: 2276–2283.

Gibson, D. G., L. Young, R. Y. Chuang, J. C. Venter, C. A. Hutchison 3rd, and H. O. Smith. 2009. "Enzymatic Assembly of DNA Molecules up to Several Hundred Kilobases." *Nature Methods* 6: 343–345.

Hanahan, D. 1983. "Studies on Transformation of *Escherichia coli* With Plasmids." *Journal of Molecular Biology* 166: 557–580.

Howerton, A., N. Ramirez, and E. Abel-Santos. 2011. "Mapping Interactions Between Germinants and *Clostridium difficile* Spores." *Journal of Bacteriology* 193: 274–282.

Jumper, J., R. Evans, A. Pritzel, et al. 2021. "Highly Accurate Protein Structure Prediction With AlphaFold." *Nature* 596: 583–589.

Kevorkian, Y., and A. Shen. 2017. "Revisiting the Role of Csp Family Proteins in Regulating *Clostridium difficile* Spore Germination." *Journal of Bacteriology* 199, no. 22: e00266-17. https://doi.org/10.1128/jb.00266-17.

Kevorkian, Y., D. J. Shirley, and A. Shen. 2016. "Regulation of *Clostridium difficile* Spore Germination by the CspA Pseudoprotease Domain." *Biochimie* 122: 243–254.

Kirk, J. A., and R. P. Fagan. 2016. "Heat Shock Increases Conjugation Efficiency in *Clostridium difficile*." *Anaerobe* 42: 1–5.

Kuwana, R., N. Okuda, H. Takamatsu, and K. Watabe. 2006. "Modification of GerQ Reveals a Functional Relationship Between Tgl and YabG in the Coat of *Bacillus subtilis* Spores." *Journal of Biochemistry* 139: 887–901.

Lord, S. J., K. B. Velle, R. D. Mullins, and L. K. Fritz-Laylin. 2020. "SuperPlots: Communicating Reproducibility and Variability in Cell Biology." *Journal of Cell Biology* 219, no. 6: e202001064. https://doi.org/10.1083/jcb.202001064.

Marini, E., C. Olivença, S. Ramalhete, et al. 2023. "A Sporulation Signature Protease Is Required for Assembly of the Spore Surface Layers, Germination and Host Colonization in *Clostridioides difficile*." *PLoS Pathogens* 19: e1011741.

McAllister, K. N., L. Bouillaut, J. N. Kahn, W. T. Self, and J. A. Sorg. 2017. "Using CRISPR-Cas9-Mediated Genome Editing to Generate *C. difficile* Mutants Defective in Selenoproteins Synthesis." *Scientific Reports* 7: 14672.

Nerber, H. N., M. Baloh, and J. A. Sorg. 2023. "The Small Acid-Soluble Proteins of *Clostridioides difficile* Regulate Sporulation in a SpoIVB2-Dependent Manner." *bioRxiv*: 2023.2005.2017.541253 20, no. 8: e1012507. https://doi.org/10.1371/journal.ppat.1012507.

Ng, Y. K., M. Ehsaan, S. Philip, et al. 2013. "Expanding the Repertoire of Gene Tools for Precise Manipulation of the *Clostridium difficile* Genome: Allelic Exchange Using pyrE Alleles." *PLoS One* 8: e56051.

Paredes-Sabja, D., P. Setlow, and M. R. Sarker. 2011. "Germination of Spores of Bacillales and Clostridiales Species: Mechanisms and Proteins Involved." *Trends in Microbiology* 19: 85–94.

Paredes-Sabja, D., A. Shen, and J. A. Sorg. 2014. "*Clostridium difficile* Spore Biology: Sporulation, Germination, and Spore Structural Proteins." *Trends in Microbiology* 22: 406–416.

Pereira, F. C., L. Saujet, A. R. Tome, et al. 2013. "The Spore Differentiation Pathway in the Enteric Pathogen *Clostridium difficile*." *PLoS Genetics* 9: e1003782.

Permpoonpattana, P., J. Phetcharaburanin, A. Mikelsone, et al. 2013. "Functional Characterization of *Clostridium difficile* Spore Coat Proteins." *Journal of Bacteriology* 195: 1492–1503.

Permpoonpattana, P., E. H. Tolls, R. Nadem, S. Tan, A. Brisson, and S. M. Cutting. 2011. "Surface Layers of *Clostridium difficile* Endospores." *Journal of Bacteriology* 193: 6461–6470.

Pizarro-Guajardo, M., P. Calderón-Romero, A. Romero-Rodríguez, and D. Paredes-Sabja. 2020. "Characterization of Exosporium Layer Variability of *Clostridioides difficile* Spores in the Epidemically Relevant Strain R20291." *Frontiers in Microbiology* 11: 1345.

Pizarro-Guajardo, M., V. Olguin-Araneda, J. Barra-Carrasco, C. Brito-Silva, M. R. Sarker, and D. Paredes-Sabja. 2014. "Characterization of the Collagen-Like Exosporium Protein, BclA1, of *Clostridium difficile* Spores." *Anaerobe* 25: 18–30.

Putnam, E. E., A. M. Nock, T. D. Lawley, and A. Shen. 2013. "SpoIVA and SipL Are *Clostridium difficile* Spore Morphogenetic Proteins." *Journal of Bacteriology* 195: 1214–1225.

Ramirez, N., M. Liggins, and E. Abel-Santos. 2010. "Kinetic Evidence for the Presence of Putative Germination Receptors in *Clostridium difficile* Spores." *Journal of Bacteriology* 192: 4215–4222.

Rohlfing, A. E., B. E. Eckenroth, E. R. Forster, et al. 2019. "The CspC Pseudoprotease Regulates Germination of *Clostridioides difficile* Spores in Response to Multiple Environmental Signals." *PLoS Genetics* 15: e1008224.

Saujet, L., F. C. Pereira, M. Serrano, et al. 2013. "Genome-Wide Analysis of Cell Type-Specific Gene Transcription During Spore Formation in *Clostridium difficile*." *PLoS Genetics* 9: e1003756.

Sebaihia, M., B. W. Wren, P. Mullany, et al. 2006. "The Multidrug-Resistant Human Pathogen *Clostridium difficile* Has a Highly Mobile, Mosaic Genome." *Nature Genetics* 38: 779–786.

Shrestha, R., A. M. Cochran, and J. A. Sorg. 2019. "The Requirement for Co-Germinants During *Clostridium difficile* Spore Germination Is Influenced by Mutations in yabG and cspA." *PLoS Pathogens* 15: e1007681.

Shrestha, R., S. W. Lockless, and J. A. Sorg. 2017. "A *Clostridium difficile* Alanine Racemase Affects Spore Germination and Accommodates Serine as a Substrate." *Journal of Biological Chemistry* 292: 10735–10742.

Shrestha, R., and J. A. Sorg. 2018. "Hierarchical Recognition of Amino Acid Co-Germinants During *Clostridioides difficile* Spore Germination." *Anaerobe* 49: 41–47.

Shrestha, R., and J. A. Sorg. 2019. "Terbium Chloride Influences *Clostridium difficile* Spore Germinastion." *Anaerobe* 58: 80–88.

Smits, W. K., D. Lyras, D. B. Lacy, M. H. Wilcox, and E. J. Kuijper. 2016. "*Clostridium difficile* Infection." *Nature Reviews. Disease Primers* 2: 16020.

Sorg, J. A., and A. L. Sonenshein. 2008. "Bile Salts and Glycine as Cogerminants for *Clostridium difficile* Spores." *Journal of Bacteriology* 190: 2505–2512.

Sorg, J. A., and A. L. Sonenshein. 2009. "Chenodeoxycholate Is an Inhibitor of *Clostridium difficile* Spore Germination." *Journal of Bacteriology* 191: 1115–1117.

Takamatsu, H., A. Imamura, T. Kodama, K. Asai, N. Ogasawara, and K. Watabe. 2000. "The yabG Gene of *Bacillus subtilis* Encodes a Sporulation Specific Protease Which Is Involved in the Processing of Several Spore Coat Proteins." *FEMS Microbiology Letters* 192: 33–38.

Takamatsu, H., T. Kodama, A. Imamura, et al. 2000. "The *Bacillus subtilis* yabG Gene Is Transcribed by SigK RNA Polymerase During Sporulation, and yabG Mutant Spores Have Altered Coat Protein Composition." *Journal of Bacteriology* 182: 1883–1888.

Theriot, C. M., M. J. Koenigsknecht, P. E. Carlson Jr., et al. 2014. "Antibiotic-Induced Shifts in the Mouse Gut Microbiome and Metabolome Increase Susceptibility to *Clostridium difficile* Infection." *Nature Communications* 5: 3114.

Varadi, M., D. Bertoni, P. Magana, et al. 2024. "AlphaFold Protein Structure Database in 2024: Providing Structure Coverage for Over 214 Million Protein Sequences." *Nucleic Acids Research* 52: D368–D375.

Wilson, K. H. 1983. "Efficiency of Various Bile Salt Preparations for Stimulation of *Clostridium difficile* Spore Germination." *Journal of Clinical Microbiology* 18: 1017–1019.

Wilson, K. H., M. J. Kennedy, and F. R. Fekety. 1982. "Use of Sodium Taurocholate to Enhance Spore Recovery on a Medium Selective for *Clostridium difficile*." *Journal of Clinical Microbiology* 15: 443–446.

Yamazawa, R., R. Kuwana, K. Takeuchi, H. Takamatsu, Y. Nakajima, and K. Ito. 2022. "Identification of the Active Site and Characterization of a Novel Sporulation-Specific Cysteine Protease YabG From *Bacillus subtilis*." *Journal of Biochemistry* 171: 315–324.

Zar, F. A., S. R. Bakkanagari, K. M. Moorthi, and M. B. Davis. 2007. "A Comparison of Vancomycin and Metronidazole for the Treatment of *Clostridium difficile*-Associated Diarrhea, Stratified by Disease Severity." *Clinical Infectious Diseases* 45: 302–307.

Zhu, D., J. A. Sorg, and X. Sun. 2018. "*Clostridioides difficile* Biology: Sporulation, Germination, and Corresponding Therapies for *C. difficile* Infection." *Frontiers in Cellular and Infection Microbiology* 8: 29. https://doi.org/10.3389/fcimb.2018.00029.

Supporting Information

Additional supporting information can be found online in the Supporting Information section.